A Simplified Approach for Anisotropic Susceptibility Map Calculation

S. Wharton[1], and R. Bowtell[1]
[1]Sir Peter Mansfield Magnetic Resonance Centre, University of Nottingham, Nottingham, United Kingdom

Introduction: Phase images of the human brain acquired using gradient echo techniques show excellent contrast resulting from differences in magnetic susceptibility across tissues [1]. Recently, it has been shown that the magnetic susceptibility of white matter (WM) has a measurable anisotropy [2-3] and Liu et al. [3] introduced a method for quantifying this anisotropy by combining phase data measured with the sample (an *ex vivo* mouse brain) positioned at 19 different orientations to the main magnetic field. In this method, field values derived from the phase data were used in a 6 parameter fit to populate the elements of a symmetric 3x3 susceptibility tensor matrix at each voxel. Here, we present a method for reducing the number of parameters in the fitting process to two, based on the assumption of cylindrical symmetry and *a priori* knowledge of the orientation of the principal axis of the susceptibility tensor. Using simulations, we demonstrate the improved conditioning that a 2-parameter fit offers relative to a 6-parameter fit for mapping anisotropic magnetic susceptibility. The development of this approach is motivated by the observations that nerve fibres in WM show local cylindrical symmetry and their orientations can be established using diffusion tensor imaging [4], making the proposed approach a viable one for measuring anisotropic susceptibility in the brain. The method could open up prospects for *in-vivo* measurements of anisotropic susceptibility, where the range of head orientations at which phase maps can be measured is limited by restrictions on subjects' head movements and the need to limit scanning times.

Theory: Figure 1 shows the geometry of the problem. In the scanner's frame of reference, the orientation of the principal axis of the Cylindrically Symmetric Susceptibility Tensor (CSST) is defined by the angles θ_T and ϕ_T and the principal components of the susceptibility tensor are written as χ_{11} and χ_{22}. In the frame of reference defined by the principal axes of the susceptibility tensor, the magnetisation is given by $\mathbf{M} = \underline{\underline{\chi}}\mathbf{H}$, where $\underline{\underline{\chi}} = \begin{bmatrix} \chi_{22} & 0 & 0 \\ 0 & \chi_{22} & 0 \\ 0 & 0 & \chi_{11} \end{bmatrix}$

To first order in χ, the magnetisation in this frame is then given by $\mathbf{M} = H_0\left[-\chi_{22}\left(\sin\theta_T\left(\cos\phi_T\hat{\mathbf{x}} + \sin\phi_T\hat{\mathbf{y}}\right)\right) + \chi_{11}\cos\theta_T\hat{\mathbf{z}}\right]$, where $H_0 = B_0/\mu_0$. Transforming back to the laboratory frame and using the substitutions $\chi_{Sum} = (\chi_{11}+\chi_{22})/2$, and $\chi_{Diff} = (\chi_{11}-\chi_{22})/2$, the components of the magnetization are found to be $M_z = H_0\left(\chi_{Sum} + \chi_{Diff}\cos 2\theta_T\right)$, $M_x = H_0\left(\chi_{Diff}\sin 2\theta_T\cos\phi_T\right)$, $M_y = H_0\left(\chi_{Diff}\sin 2\theta_T\sin\phi_T\right)$. We can now calculate the *z*-component, B_z, of the field perturbation produced by the induced magnetisation. In doing this, the *x* and *y*-components of the magnetization cannot be ignored as they contribute to B_z. By transforming the problem to the Fourier domain and using a spherical harmonic expansion, we find that B_z due to the CSST is given by Eq.[1]. Here θ_k and ϕ_k are the spherical polar coordinates of **k** in the frame defined with B_0 parallel to *z* (Fig. 1). Equation [1] can be used to calculate the field offset due to a CSST based on knowledge of: the direction of the principal axis and parameters describing the sum and difference of the two susceptibility values. It can also be used in solving the inverse problem in which the components of the CSST are calculated from measurements of B_z.

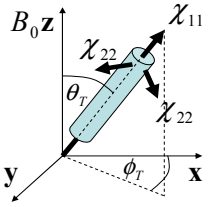

Fig.1 Schematic of CSST.

$$B_z(\mathbf{k})/B_0 = FT\left(\chi_{Sum} + \chi_{Diff}\cos 2\theta_T\right)\times\left(\cos^2\theta_k - 1/3\right) + FT\left(\chi_{Diff}\sin 2\theta_T\cos\phi_T\right)\times\left(\sin 2\theta_k\cos\phi_k\right)/2 + FT\left(\chi_{Diff}\sin 2\theta_T\sin\phi_T\right)\times\left(\sin 2\theta_k\sin\phi_k\right)/2 \quad \textbf{Eq.1}$$

Methods: To validate the theory, the field offset due to a simulated CSST was calculated using both Eq.[1] and the previously described, 6 parameter (6P) forward calculation [3].A numerical phantom consisting of two ellipsoids containing materials characterised by different CSST's was used. One ellipsoid (EA) contained material with a principal axis oriented along *z,* while the material of the second ellipsoid (EB) had a principal axis oriented along *y*. We set χ_{11} =2 and χ_{22} = 1 in both ellipsoids and B_0 was oriented along *z*. Fig.2a shows the orientations of the CSST's for each ellipsoid, and Fig.2b shows the simulated field from the 6P forward calculation. The field calculated for the same arrangement using the 2-parameter (2P) forward calculation (Eq.[1]) is shown in Fig. 2c. The difference in the two simulations, Fig.2b-Fig.2c, was negligible. The next stage was to invert the validated 2P forward calculation to reconstruct a susceptibility map, and to compare with the results of the 6P inversion [3]. The ill-posed inversion can be conditioned by combining data sampled with different object orientations relative to B_0. To test the level of conditioning required by the 2P and 6P methods, three different orientation sampling strategies were considered: 1-20 orientations restricted to a range of motion (ROM) of ±20° from a neutral position (this is the estimated maximum ROM for a human subject inside an MRI scanner), 1-20 orientations with an ROM of ±40°, and 1-20 orientations with an ROM of ±60°. One sampling strategy (20 orientations with an ROM of ±40°) is depicted in Fig.3. In each case, the sampling axes were approximately evenly spread over the surface defined by the ROM. The inversion was carried out using a conjugate gradient method [5], based on either the 2P or 6P forward calculations and limited to 50 iterations. For each sampling strategy χ_{11} and χ_{22} maps were calculated and an error % was formed relative to the actual values.

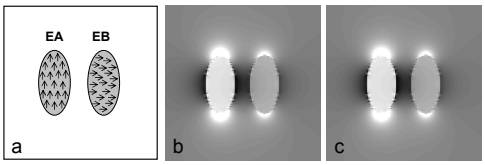

Fig.2 Simulated fields due to two CSST's (a), using the 6P method (b) and the 2P method (c).

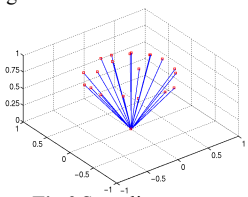

Fig.3 Sampling strategy for ROM =±40°.

Results and Discussion: Table 1 details the minimum number of orientations, N_O, that the 2P and 6P methods needed to reconstruct χ_{11}& χ_{22} susceptibility maps with a mean error of less than 10% and 5% for the different ROM values. Representative slices of the reconstructed χ_{11} maps are shown in Fig.4 for: the 6P method with ROM/N_o= ±20°/3 (Fig.4a) & ±60°/6 (Fig.4b) and the 2P method with ROM/ N_o= ±20°/3 (Fig.4c) & ±20°/5 (Fig.4d). These show that the 2P method can produce good quality maps of χ_{11} & χ_{22} with a lower number of orientations and a smaller range of motion than required by the 6P method. When the number of samples or ROM is too small the 6P method underestimates the value of χ_{11} in compartment EB where the principal axis is perpendicular to B_0. In These results indicate that high quality CSST maps can be created using 5 sampling orientations spread over a ±20° ROM. This is an important finding as it suggests that given *a priori* knowledge of the spatial variation of the CSST orientation (e.g. from DTI data), maps of anisotropic susceptibility could be produced *in–vivo* where the number and range of head orientations that can be measured is limited. In conclusion, we have presented and validated a 2-parameter method for calculating the field offsets produced by a distribution of cylindrically symmetric anisotropic susceptibility and have shown that this method allows mapping of susceptibility anisotropy using a relatively small number of measurements. This opens up the possibility of exploiting anisotropic susceptibility mapping in clinical studies.

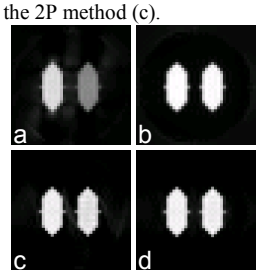

Fig.4 χ_{11} maps for: (a) 6P,±20°,N_o=3; (b) 6P,± 60°,N_o=6 ; (c) 2P±20°,N_o=3;)(d) 2P±20°,N_o=5.

Regime	ROM	N_0 (error ≤10%)	N_o (error ≤5%)
6P	±20°	6	-
	±40°	7	9
	±60°	6	6
2P	±20°	3	5
	±40°	3	4
	±60°	3	4

Table.1 Results for 2P vs 6P inversion.

References: [1] Duyn at al. 2007. PNAS.104:11796-11801,[2] Lee at al. 2010. PNAS.107:5130-5135,[3] Liu, C. 2010. MRM. 63:1471-1477,[4] Mori et al. 2006. AJNR. 27:1384-1385, [5] Hestenes et al. 1952. JRNBS. 49:409.